Dynamics in coarse-grained models for oligomer-grafted silica nanoparticles

Bingbing Hong, Alexandros Chremos, and Athanassios Z. Panagiotopoulos

Citation: The Journal of Chemical Physics **136**, 204904 (2012); doi: 10.1063/1.4719957
View online: http://dx.doi.org/10.1063/1.4719957
View Table of Contents: http://scitation.aip.org/content/aip/journal/jcp/136/20?ver=pdfcov
Published by the AIP Publishing

Dynamics in coarse-grained models for oligomer-grafted silica nanoparticles

Bingbing Hong, Alexandros Chremos, and Athanassios Z. Panagiotopoulos[a)]
Department of Chemical and Biological Engineering, Princeton University, Princeton, New Jersey 08544, USA

(Received 24 February 2012; accepted 4 May 2012; published online 30 May 2012)

Coarse-grained models of poly(ethylene oxide) oligomer-grafted nanoparticles are established by matching their structural distribution functions to atomistic simulation data. Coarse-grained force fields for bulk oligomer chains show excellent transferability with respect to chain lengths and temperature, but structure and dynamics of grafted nanoparticle systems exhibit a strong dependence on the core-core interactions. This leads to poor transferability of the core potential to conditions different from the state point at which the potential was optimized. Remarkably, coarse graining of grafted nanoparticles can either accelerate or slowdown the core motions, depending on the length of the grafted chains. This stands in sharp contrast to linear polymer systems, for which coarse graining always accelerates the dynamics. Diffusivity data suggest that the grafting topology is one cause of slower motions of the cores for short-chain oligomer-grafted nanoparticles; an estimation based on transition-state theory shows the coarse-grained core-core potential also has a slowing-down effect on the nanoparticle organic hybrid materials motions; both effects diminish as grafted chains become longer. © *2012 American Institute of Physics*. [http://dx.doi.org/10.1063/1.4719957]

I. INTRODUCTION

Nanoparticle organic hybrid materials (NOHMs) consist of inorganic nanoparticles covalently grafted with oligomer chains. They display liquid-like rheological behavior around room temperature in the absence of solvent.[1–3] Properties of NOHMs are determined by interactions and motions that span a wide range of length and time scales, as is also the case for particle nanocomposites, the ungrafted counterparts of NOHMs. Although models with atomistic descriptions of both nanoparticles and chains have been developed for nanocomposites,[4–8] their application is often limited to systems with one nanoparticle, and they can only provide information on local polymer structures (length scales <4 nm) over short times of the order of ns. In order to describe larger-scale properties such as nanoparticle dispersion and transport, a NOHMs model with solid-sphere nanoparticles and atomistic polymers was recently proposed that is suitable for simulating systems consisting of hundreds of nanoparticles.[9] However, slow dynamics of nanoparticle motions preclude a direct application of the model to NOHMs near room temperature. Coarse-grained models with reduced number of degrees of freedom and improved computation efficiency are potentially useful tools to allow for exploration of bulk properties of NOHMs using current computational capabilities.

Many existing coarse-grained models for nanoparticle/polymer systems are qualitative in character, with no connections to the atomistic chemistry of specific experimental systems.[10,11] Such models have been used to investigate morphologies,[12–14] structure and dynamics,[15–19] mechanical properties,[20–22] and rheological behavior[21,23] of nanocomposites, grafted nanoparticles in a polymer matrix, and NOHMs. Coarse-grained models that couple to the underlying atomistic descriptions are primarily used in modeling properties in polymeric systems, such as configurations and dynamics in the melt[11,24–27] and solutions,[28,29] polymer brush conformations,[30] self-assembly kinetics,[31] etc. To our knowledge, there is only one prior study that has used multiscale modeling for a simplified system of nanocomposites focusing on how to improve the coarse-grained parameters to match nanoparticle distributions obtained by atomistic models.[10] Thus, there is significant room for further development of parameterization techniques and mapping schemes for structure and dynamics between coarse-grained and atomistic levels in nanoparticle/polymer simulations. This is the focus of the present work.

For polymer systems, it is well known that dynamical properties, e.g., diffusion coefficients and chain relaxations, are faster in the coarse-grained models than the atomistic reference systems.[11,24,26–28,32] This is attributed to the softer coarse-grained potentials, which reduce local friction and energy barriers, accelerating the cage escape of diffusing molecules.[25,26] Depa *et al.* performed mappings for a series of polymer materials and found that atomistic dynamics could be recovered after a crossover time by rescaling of the mean-square displacements (MSD). However, the scale factors varied, depending on state conditions and material chemistry.[11,26,27] In analogy to the accelerated molecular dynamics for infrequent events via an introduction of a bias potential,[33] Depa and Maranas[27] and Fritz *et al.*[25] proposed that the speed-up (scale factor) of dynamics in coarse-grained models compared with the underlying atomistic systems is

$$\alpha_b = \exp\left(\langle \Delta V_b \rangle / k_B T\right), \tag{1}$$

where the bias potential, $\langle \Delta V_b \rangle$, is the ensemble average of the difference between the potentials of coarse-grained

a)Electronic mail: azp@princeton.edu.

TABLE I. Simulation details for atomistic and coarse-grained PEO oligomers.

n-mer (atomistic)	N chains	n-bead (coarse-grained)	N chains	Number density of molecules (nm^{-3})	
				303 K	500 K
1	216	1	1000	5.728	…
3	216	2	500	3.300	2.480
5	200	3	400	2.307	1.820
…	…	4	300	1.772[a]	…
9	150	5	300	1.438	1.169
…	…	6	200	1.211[a]	0.9900[a]
12	100	…	…	1.122	0.9172
…	…	7	200	1.043[a]	0.8800[a]
…	…	10	200	0.7333[a]	…
…	…	20	150	0.3675[a]	…

[a]Obtained by interpolation and extrapolation of number densities of chains in atomistic simulations.

particle and the atomistic atom groups the particle represents. $\langle \Delta V_b \rangle$ is mainly determined by the potential differences at the first layer of particles that surrounds the central particle. When such mapping of dynamical properties can be established, acceleration of dynamics for coarse-grained simulations offers the advantage that long-time behavior can be obtained at a modest computational cost.[25,26,34] However, it is unclear that such dynamic scaling relationships can be obtained in more complex particle/chain composite systems. This is an open question of interest for the present study.

Poly(ethylene oxide) (PEO, CH_3O–$(CH_2CH_2O)_n$–CH_3) oligomer chains and silica nanoparticles are typical constituents for NOHMs in experimentally studied systems. In this work, we develop a structure-based coarse-grained model for silica nanoparticles grafted with oligomeric PEO chains from atomistic reference systems of oligomers[35] and NOHMs bulk systems.[9] In Sec. II of this paper, we describe how the coarse-grained models for pure oligomers and NOHMs are constructed. Structural and dynamic properties are described in Sec. III. Coarse-graining PEO oligomer melts results in faster dynamics, in accordance with prior simulations mentioned above. However, counterintuitive results are observed for diffusion of nanoparticles in coarse-grained models with unchanged inter-core potentials or with short grafted chains: diffusion coefficients become *smaller* compared to corresponding atomistic simulations. We examine the effect of potential softness and grafting topology to gain insights into the causes of slower diffusion of coarse-grained nanoparticles. Conclusions are presented in Sec. IV.

II. COARSE-GRAINED MODEL DEVELOPMENT

The coarse-grained NOHMs are composed of two types of interaction sites, one for polymer beads, each of which represents one segment of PEO oligomer chains, and the other for the central cores representing nanoparticles. From this point on, "segments" and "nanoparticles" are only used for the reference atomistic systems, and their counterparts in the coarse-grained models are termed "beads" and "cores." We parameterize the bead-bead interactions, bond, and angle parameters using atomistic simulations of bulk oligomers. Core-bead potentials are determined from systems of one nanoparticle immersed in monomers. For core-core potentials, we use both the atomistic particle-particle potential and the potential corrected for changes in the polymer-mediated interactions between two nanoparticles brought about by coarse-graining of oligomers.

A. Bulk oligomers

The atomistic models of PEO oligomers used in this work have been previously described in Ref. 35. They involve transferable potentials for phase equilibria-united atom (TraPPE-UA) force fields with modified dihedral potentials.[28] We have performed NVT simulations of atomistic oligomers at two temperatures, 303.15 K and 500 K, with densities set corresponding to 10 bar at each temperature (Table I). The production periods for short to long atomistic oligomers were 2–40 ns at 303.15 K and 3–12 ns at 500 K with a time step of 2 fs.

To construct coarse-grained models, all united atoms in two consecutive $–(CH_2OCH_2)–$ units were grouped into one electrostatically neutral bead. Differences in size, mass, and interactions by the third hydrogen in the end $–CH_3$ group were neglected. Then, each atomistic n-mer molecule is represented by one $\frac{1}{2}(n+1)$-bead chain. The non-bonded potential between beads was obtained from iterative Boltzmann inversion[28,32,36,37] by matching the radial distribution function, $g_{bb}(r)$, of a monomeric bead melt with that of pure atomistic monomers at 303 K. The initial potential was taken to be the potential-of-mean-force for atomistic monomers, $U_{\rm pm} = -k_{\rm B}T \ln g_{\text{1-mer}}(r)$, with a cut-off radius at $r_c = 1.6$ nm. The production period for each iteration was 4 ns. Although the iterative Boltzmann inversion method is not rigorously derived from statistical mechanics as is the case for inverse Monte Carlo[38,39] and relative entropy minimization,[40,41] it has the advantages of low computational costs and easy implementation – especially for large molecules. Figure 1 illustrates the bead-bead non-bonded coarse-grained potential and a good correspondence of $g_{bb}(r)$ between atomistic and coarse-grained models.

We used harmonic bonds, $U_b(r) = k_b(r - r_0)^2$, to connect beads into chains, where the equilibrium distance $r_0 = 0.585$ nm was determined by fitting the mean-squared bond length of 2-bead chains to the mean-squared distance between

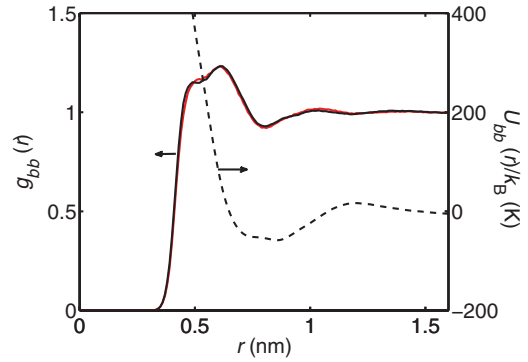

FIG. 1. Non-bonded potential between coarse-grained beads and comparison of bead-bead radial distribution function, $g_{bb}(r)$, between atomistic and coarse-grained simulations of monomers at 303 K. Red solid line: segment-segment atomistic $g_{ss}(r)$; black solid line: coarse-grained $g_{bb}(r)$; black dashed line: coarse-grained non-bonded potential.

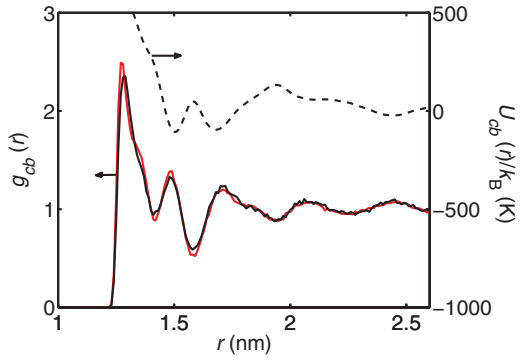

FIG. 2. Non-bonded potential between the core and coarse-grained beads, and the core-bead radial distribution functions for systems of single nanoparticles in atomistic and coarse-grained monomers, $g_{cb}(r)$, at 303 K. Red solid line: atomistic $g_{ps}(r)$; black solid line: coarse-grained $g_{cb}(r)$; black dashed line: coarse-grained non-bonded potential.

centers of mass of the two segments (CH_2OCH_2–CH_2OCH_2 groups) in atomistic trimers. With given r_0, the value $k_b = 477\,\text{kJ/(mol nm}^2)$ was then obtained through minimization of the difference between the distance distribution of two bonded beads and that of two sequential atomistic segments. The persistence length, P, for atomistic PEO is approximately equal to 3 bonds, and was obtained through the expression $\langle r_{ee}^2 \rangle = 2P^2 \left[L/P - 1 + \exp\left(-L/P\right) \right]$,[42] where $\langle r_{ee}^2 \rangle$ is the mean square of end-to-end ($–CH_3$ to $–CH_3$) distance, and the contour length, L, was calculated as the summation of bond lengths along the chain backbone. These calculations indicated that two consecutive CH_2OCH_2 groups (one coarse-grained bead) cannot rotate independently, so it is necessary to incorporate angle potentials in the coarse-grained model. We successively adjusted θ and k_θ for an angle potential of the form $U_\theta = k_\theta(\theta - \theta_0)^2$, so that the end-to-end distance, $\langle r_e^2 \rangle$, of 6-bead chains matched the corresponding value of end-segment to end-segment distance for atomistic PEO, and the difference between the angle distributions of 3-bead chains and atomistic pentamers was minimized. The process was repeated two to three times because θ and k_θ are not independent; the final values were $\theta = 155^\circ$ and $k_\theta = 4.60\,\text{kJ/(mol radian}^2)$. Tabulated bond and angle potentials could be developed for the coarse-grained model to further improve the bond and angle distributions, but such changes are expected to have only minor effect on the chain dynamics.

Prior studies[28,29,31,43] have shown that coarse-grained systems have higher pressures than the atomistic counterparts at the same density, due to the higher fraction of free ends in a coarse-grained oligomer melt. The overestimated isothermal compressibility[24] suggests low transferability of the coarse-grained force fields in reproducing the densities of atomistic models when temperature changes. Thus, we set the number densities of chains in coarse-grained models to be the same as those of corresponding atomistic systems, as shown in Table I. Simulations were performed under constant-volume conditions, coupled with Nosé-Hoover thermostats for temperature control, using the LAMMPS package.[44,45] The time step was 2 fs for all the coarse-grained models, including bulk polymers, ungrafted nanoparticle in free chains, and NOHMs, and the total simulation time was 8–20 ns for 1- to 20-bead chains at 303 K and from 4 to 8 ns for 2- to 7-bead chains at 500 K.

B. Ungrafted nanoparticle in oligomers

Systems of a single ungrafted nanoparticle in 8890 free monomers were simulated as the reference for the development of core-bead interactions, $U_{cb}(r)$. The nanoparticle was represented by a solid sphere of diameter $d = 2$ nm interacting with united atoms through integrated Lennard-Jones (LJ) potentials. The second part of Ref. 9 gives the details of the models of nanoparticles in free oligomers. For these systems and the grafted systems described in Sec. II C, we used finitely extensible nonlinear elastic (FENE) bonds (rather than the rigid bonds of Sec. II A), and the time step was set to 0.5 fs.[9] The system density was equilibrated under constant-pressure conditions at 303 K and 1 bar before runs in the NVT ensemble were performed. The equilibrated box size (10.91 nm) was larger than twice the cutoff of particle-particle interaction, $r_c = 5$ nm. The coarse-grained systems had the same number of molecules and total density as the atomistic models. Following Khounlavong's procedure of coarse-graining particle nanocomposite systems,[10] we parameterized the core-bead interactions through matching of core-bead radial distribution functions, $g_{cb}(r)$, between atomistic and coarse-grained scales. The iterative Boltzmann inversion method was implemented again with the initial guess for core-bead interaction chosen as $U_{cb,0}(r) = -k_B T \ln g_{ps}(r)$. Here, $g_{ps}(r)$ is the nanoparticle-monomer radial distribution function of the single nanoparticle atomistic system. The simulation time for each iteration of the coarse-grained model was 10 ns. Figure 2 presents the core-bead interaction from the last iteration and compares the converged coarse-grained $g_{cb}(r)$ with the atomistic radial distribution function.

C. Grafted solvent-free particles (NOHMs)

With U_{bb} and U_{cb} developed in Secs. II A and II B, we constructed the core-core interactions, $U_{cc}(r)$, by matching the core-core radial distribution functions, $g_{cc}(r)$, between coarse-grained and atomistic NOHMs. The atomistic NOHMs used

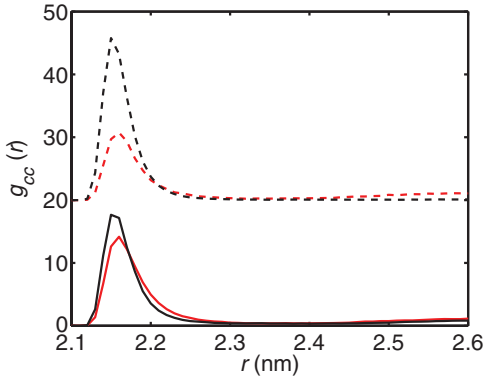

FIG. 3. Core-core radial distribution functions, $g_{cc}(r)$, of NOHMs at 500 K with cores interacting through the particle-particle potential, $U_{pp}(r)$, from atomistic models. Red solid line: atomistic $g_{pp}(r)$ for pentamer-grafted NOHMs; black solid line: coarse-grained $g_{cc}(r)$ for 3-bead-grafted NOHMs; red dashed line: atomistic $g_{pp}(r)$ for tridecamer-grafted NOHMs (shifted upwards by 20 units); black dashed line: coarse-grained $g_{cc}(r)$ for 7-bead-grafted NOHMs (shifted upwards by 20 units).

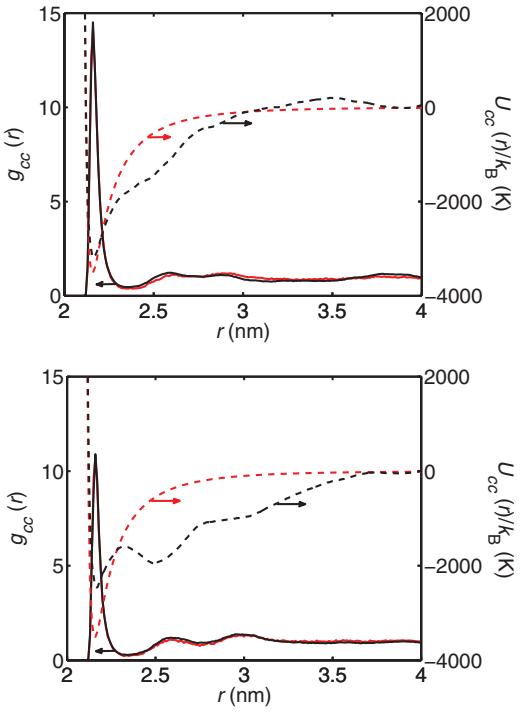

FIG. 4. Radial distribution functions between cores of NOHMs that interact with corrected core-core interactions. Top: NOHMs with pentamers or 3-bead chains at 500 K. Bottom: NOHMs with tridecamers or 7-bead chains at 500 K. Red solid line: atomistic $g_{pp}(r)$; black solid line: coarse-grained $g_{cc}(r)$; red dashed line: atomistic particle-particle potentials; black dashed line: corrected inter-core potentials.

as the reference consisted of one $d = 2$ nm central silica nanoparticle represented by a solid sphere and 12 covalently grafted hexamers or dodecamers (about 0.9 chains/nm^2). Nanoparticles interact with each other and other united atoms in oligomers through integrated LJ potentials. The model was established and described in Ref. 9 and has been shown to reproduce experimental viscosity data. Due to the slow relaxation of nanoparticle motions, atomistic simulations were performed at 500 K and above. Consequently, coarse-graining of NOHMs in this paper was conducted at 500 K as well, after the transferability of the coarse-grained force fields for polymer beads was tested.

The coarse-grained NOHMs are comprised of a solid-sphere core and grafted PEO oligomers. Essentially only the chains are coarse-grained and the cores remain the same as the nanoparticles in atomistic NOHMs. Khounlavong *et al.* have reported for particle nanocomposites, coarse-graining chains alters the potential of mean force between the nanoparticles and therefore the inter-core interactions should be modified accordingly.[10] Figure 3 illustrates how the core-core radial distributions, $g_{cc}(r)$, agree with the nanoparticle distributions in atomistic models if the core-core interactions are set equal to the particle-particle potentials in the atomistic reference NOHMs. Compared with the large deviations in the peak positions and heights before adding a correction of polymer-mediated force to the atomistic core-core interactions as in the work of Khounlavong *et al.* (Fig. 7 in Ref. 10), the differences between the coarse-grained and atomistic $g_{cc}(r)$s of NOHMs we obtain are relatively small, especially for shorter chains. As the grafted chains grow longer, the discrepancies of coarse-grained and reference $g_{cc}(r)$s become larger. This chain-length dependence was also observed in Kahounlavong *et al.* simulations.

In Ref. 10, the core-core potential was taken as the atomistic particle-particle potential modified by addition of the change in the polymer-mediated force before and after coarse-graining, $U_{cc}(r) = U_{pp}(r) + U_{pm,CG}(r) - U_{pm,at}(r)$, where $U_{pm,at}$ and $U_{pm,CG}$ are the potentials-of-mean-force between two nanoparticles in atomistic models and coarse-grained models, which take $U_{pp}(r)$ as the core-core interactions, respectively. The correction was essentially the first iteration of the iterative Boltzmann inversion method. In this study, we perform more iterations through

$$U_{cc}^{i+1}(r) = U_{cc}^{i}(r) + x\left(U_{pm,CG}^{i}(r) - U_{pm,at}(r)\right) \qquad (2)$$

to further enhance the convergence of the core-core radial distribution function, $g_{cc}(r)$, to the atomistic $g_{pp}(r)$. The coefficient, x, varies during the iterations to adjust the convergence speed. The final forms of $U_{cc}(r)$ and $g_{cc}(r)$ for 3-bead- and 7-bead-grafted NOHMs are presented in Fig. 4. Comparisons with the atomistic particle-particle potentials show that the corrections raise the energy wells and increase the softness of the interactions. One may think that the structural changes induced by the corrections in coarse-grained models would not affect the dynamics significantly, especially for 3-bead-grafted NOHMs where the change of $g_{cc}(r)$ is very small. However, when we use both uncorrected (reference) and corrected core-core potentials for the study of diffusion (Sec. III B) we find that the changes in dynamics can be in opposite directions.

In the atomistic simulations, the first oxygen atom of each oligomer is fixed on the surface of the nanoparticles. The coarse-grained beads attached on the central core and the core itself are treated as a rigid body in the coarse-grained simulations. Table II summarizes the atomistic and coarse-grained NOHMs systems and simulation details. Each Boltzmann inversion iteration lasted 20–40 ns for NOHMs grafted from 3- to 7-bead chains.

TABLE II. Simulation details for nanoparticles in atomistic and coarse-grained NOHMs.

N_p cores or nanoparticles	n-mer (atomistic)	n-bead (coarse-grained)	N chains (both)	Box size (nm) at 500 K
140	5	3	1680	11.92
130	6	...	1560	11.90
120	...	4	1440	11.87
90	...	6	1080	11.63
80	12	...	960	11.36
70	13	7	840	11.06

III. RESULTS

A. Bulk oligomers

We first examine the transferability of the coarse-grained force fields to bulk PEO oligomers of different chain lengths and temperatures. Figure 5 presents the radial distribution functions of the centers of mass, $g_{\rm mm}(r)$, for pentamers (3-bead chains) and nonamers (5-bead chains) at 500 K. $g_{\rm mm}(r)$s at 303 K and the agreement between atomistic and coarse-grained radial distribution functions is almost the same as for 500 K. The figure indicates that up to the temperature of simulated NOHMs, the mutual exclusion or the potential of mean force between the atomistic oligomers can still be well captured by the coarse-grained potentials. In both models, longer chains are more likely to penetrate into their neighbors, which is reflected by the non-zero $g_{\rm mm}(r)$ at short distances, r.

Figure 6 plots the chain length dependence of the end-to-end distances, $\langle r_e^2 \rangle$, of oligomers in atomistic and coarse-grained models. As the data illustrate, in the range of chain lengths used for NOHMs (from pentamers to tridecamers) coarse-grained and atomistic models generate oligomers that have almost the same average extension at 303 K, where the force fields were developed and at 500 K, to which the force fields are transferred to. Temperature has little influence on $\langle r_e^2 \rangle$. As chains grow longer, raising the temperature slightly reduces $\langle r_e^2 \rangle$. This can be attributed to the increased kinetic energy, which helps overcome the bending barriers of oligomers, making the chains less stiff.

The chain length dependence of the diffusion coefficients, D, at 303 K and 500 K, is shown in Fig. 7. The diffusion coefficients obtained from atomistic and coarse-grained models at 500 K and those from the coarse-grained model at 303 K scale similarly over the chain lengths studied, with an exponent -1.1 to -1.3, while the scaling factor for the atomistic model at 303 K is -1.9 to -2.5. The former exponents suggest that the chain behavior is close to the Rouse model in the coarse-grained models and, at high temperatures, for the atomistic models. The atomistic PEO models used here have been tested before to generate densities and viscosities in good agreement with experiments.[35] Assuming the glass transition of the atomistic oligomers is similar to what is found in experiments, the glass transition temperature is expected to be below 200 K.[9,46] The higher slope for atomistic PEO at low temperature, as seen in Fig. 7, is thus not caused by proximity to the glass transition. It is likely due to the strong atomistic interactions that limit the oligomer motions and increase the chain stiffness. Reference 47 found that n-alkanes do not exhibit ideal-chain statistics until n is greater than 100. The atomistic PEO at 303 K is in the "oligomer" regime, with chains expected to approach ideal behavior at higher chain lengths. Raising the temperature, or using softer coarse-grained potentials, moves the crossover of oligomer and ideal-chain statistics towards shorter chains.

We can also observe from Fig. 7 that diffusion of oligomers is accelerated after being coarse-grained and the

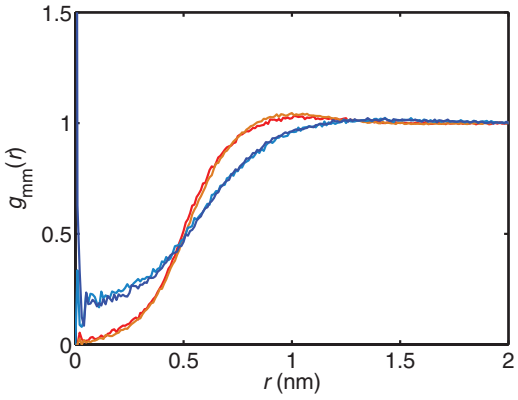

FIG. 5. Radial distribution functions of molecular centers of mass for PEO oligomers at 500 K. Red: atomistic pentamers; orange: coarse-grained 3-bead chains; darker blue: atomistic nonamers; lighter blue: coarse-grained 5-bead chains.

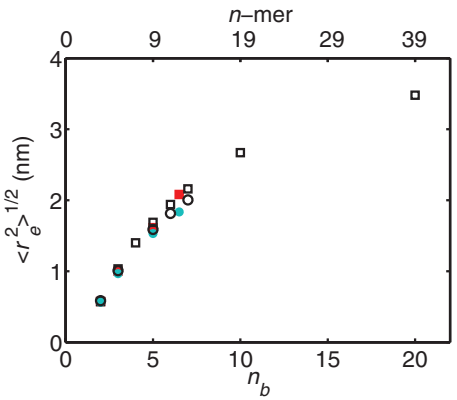

FIG. 6. The end-to-end (end segment-to-end segment) distances of oligomers at 303 K and 500 K. Red square: atomistic oligomers at 303 K; black square: coarse-grained oligomers at 303 K; red circle: atomistic oligomers at 500 K; black circle: coarse-grained oligomers at 500 K. The points calculated at both temperatures and from two levels of models almost overlap for trimers and pentamers (or 2- and 3-bead chains).

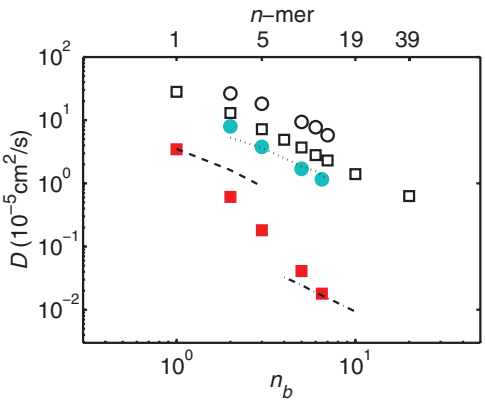

FIG. 7. The diffusion coefficients of oligomers at 303 K and 500 K. Red square: atomistic oligomers at 303 K;[35] black square: coarse-grained oligomers at 303 K; red circle: atomistic oligomers at 500 K; black circle: coarse-grained oligomers at 500 K; dashed line: $D_{cg}/8$ at 303 K; dotted-dashed line: $D_{cg}/150$ at 303 K; dotted line: $D_{cg}/5$ at 500 K.

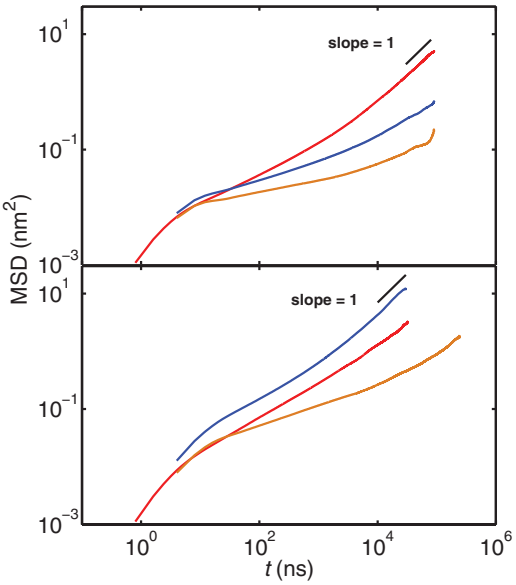

FIG. 8. The MSD of NOHMs grafted with pentamers (top) and tridecamers (bottom) at 500 K. Red line: atomistic NOHMs; orange line: coarse-grained NOHMs using uncorrected inter-core potentials; blue line: coarse-grained NOHMs using corrected core-core potentials.

speed-up ratio, $s = D_{cg}/D_{at}$, depends on the temperature and chain length. Similarly, faster dynamics were also reported in previous coarse-grained simulations of PEO solutions and melts,[28,43] polyamide melts,[24] polyethylene,[26,27] and polystyrene.[48] Figure 7 illustrates that the speed-ups become smaller when temperature is raised, as reported in Refs. 24 and 28. At high temperature, where both atomistic and coarse-grained chains show similar Rouse-like motions, there is a roughly universal speed-up for different chain lengths. In other words, as long as the chains have not entered the reptation regime, the determination of diffusivities of atomistic PEO can be easily performed by scaling the coarse-grained diffusivities using s and thus avoiding time-consuming atomistic simulations. However, at low temperature, the speed-up varies with chain length due to the different modes of motion that atomistic and coarse-grained oligomers obey. The speed-ups have to be extrapolated from Fig. 7 before mapping the coarse-grained diffusivities to the atomistic values for longer chains. Depa and other researchers did a series of multiscale simulations of polymers[11,26,27,43,48] and found that if the structures of atomistic and coarse-grained polymers match with each other, the diffusive regime of the MSD for atomistic polymer centers of mass can be recovered by rescaling the time, $\Delta t_{at} = \alpha \Delta t_{cg}$. The "indirect speed-up," α, as defined in their work, is essentially the same as s in this study. But their work reflected that structure-based coarse-graining basically changes the way and consequently the time by which the beads/segments use to escape from the cage formed by their neighbors.[26] The faster cage escape of coarse-grained beads is attributed to the softer potentials, which reduce the local friction one bead/segment experiences.[26,48,49] Depa and Maranas used united-atom and coarse-grained potentials to approximate $\langle \Delta V_b \rangle$ (Eq. (1)) of polyethylene and the estimated speed-ups, α_b, were within 7% of α or s obtained from MSD or diffusion coefficient match.[27] The estimation indicates the speed-up in structure-based coarse-graining of linear polymers is basically contributed by potential softening.

B. Grafted solvent-free particles (NOHMs)

Section II C has shown the g_{cc} data of coarse-grained and atomistic NOHMs. Here, we first examine the influence of the introduction of nanoparticles and grafting on chain dimensions. The end-to-end segment distances, $\langle r_e^2 \rangle^{1/2}$, of grafted pentamers and grafted tridecamers are 0.947 ± 0.002 nm and 1.945 ± 0.006 nm, respectively. With uncorrected atomistic particle-particle potentials employed in the coarse-grained models, the end-to-end distances of grafted 3-bead chains and 7-bead chains are 5% and 4% longer than their atomistic counterparts. Corrected core-core potentials improve the agreements to be 4% longer for short chains and within the error for long chains. The small differences between the coarse-grained and atomistic $\langle r_e^2 \rangle^{1/2}$ shows good transferability of coarse-grained core-bead and bead-bead potentials to grafted systems.

The mean square displacements of atomistic and coarse-grained NOHMs are compared in Fig. 8. First, it can be observed that coarse-graining does not alter the chain-length dependence of diffusivities for NOHMs at 500 K. The NOHMs grafted with long oligomers (tridecamers) move faster than NOHMs with short chains, because the former systems have larger core volume fractions.[9,17] Figure 8 also illustrates for both NOHMs grafted with short (pentamer) and long (tridecamer) oligomers, the cores in coarse-grained NOHMs interacting with uncorrected inter-particle potentials from atomistic models diffuse more slowly than nanoparticles in atomistic models, although all united atoms in grafted oligomers are coarse-grained into softer beads. Yet correcting the core-core potentials, which softens the atomistic potentials and generates excellent $g_{cc}(r)$ agreements between coarse-grained and atomistic NOHMs (Fig. 4), accelerates the core motions in both coarse-grained 3-bead and 7-bead-chain NOHMs. The cores grafted with long oligomers diffuse

eventually faster than nanoparticles in atomistic models, similar to the dynamics changes of coarse-grained linear polymers, while the cores with short oligomers still cannot catch up with the nanoparticle diffusion in atomistic models. This trend is promising for further development of multiscale modeling of NOHMs, in that for realistic NOHMs grafted with chains 5 to 6 times the lengths of the oligomers used in this paper, coarse-graining does not introduce extra time that needs to be spent for the slowed core diffusion which counterbalance the time saved by the reduction of interaction sites. On the other hand, comparisons between Figs. 4 and 8 reflect the high sensitivity of core dynamics upon changes of inter-core interactions. For coarse-grained NOHMs with short chains, 10% change in the potential energy well leads to around 20-fold increase in the diffusion coefficient. In contrast, a 50% raise of the energy well for pairwise potentials between two polymer beads only accelerates diffusion of polymers (∼4000 g/mol) by 2 to 5 times.[24] Both Figs. 4 and 8 indicate poor transferability of core-core potentials to coarse-grained NOHMs with other chain lengths. We also checked the atomistic and coarse-grained NOHMs at 1000 K and found unsatisfactory agreement between $g_{cc}(r)$ and $g_{\text{p-p}}(r)$. The poor transferability of coarse-grained core-core potentials to different temperatures and different chain lengths suggests that prior knowledge of atomistic distributions has to be available for development of coarse-grained force fields specific to each system at each condition. Consequently, coarse-grained models of NOHMs may lose their computational efficiency advantages over atomistic NOHMs models, unless a predictive way for construction of the core-core potentials can be found.

The dynamics of grafted chains are examined through the relaxation of square end-to-end distance correlation,

$$C_R(t) = \frac{\langle r_e^2(0) r_e^2(t)\rangle - \langle r_e^2\rangle^2}{\langle r_e^4\rangle - \langle r_e^2\rangle^2} \tag{3}$$

and are shown in Fig. 9. The decorrelation time scales for 3- and 7-bead chains are shortened about 500 and 20 times, respectively, by coarse-graining. Unlike the sensitive dependencies of the core motions on the core-core potentials, $C_R(t)$s show negligible changes, independent of whether the core-core potentials are corrected. Due to the grafting topology, complete decorrelation of $C_R(t)$ cannot be realized for atomistic oligomers. Figure 9 illustrates that $C_R(t)$ of atomistic pentamers stops decreasing further once it reaches a value of around 0.6. $C_R(t)$ of atomistic tridecamers keeps decreasing until $C_R(t)$ is reduced to about 0.25, similar to the whole chain relaxation of dodecamers reported in Ref. 9. But in coarse-grained models the softened potentials make the decorrelation of $C_R(t)$ more complete. The accelerated dynamics of coarse-grained grafted chains suggests that it is not the chain motions that induces the slow-down of core diffusion for coarse-grained NOHMs grafted with short chains.

Data for $g_{cc}(r)$ (Fig. 4) illustrate that the first minima appear around $r = 2.4$ nm in both atomistic and coarse-grained models. The nearest distance between the surfaces of any pair of neighbor particles or cores is then 0.4 nm, which is intermediate between the atom size (∼0.3 nm) and the bead size (0.65 nm, the distance at which $U_{bb}(r) = 0$). Thus, one explanation for the reason that coarse-graining induces slowed core motions in short-chain grafted systems is that the first coarse-grained beads fixed onto the core surfaces cannot change their shapes and positions, when the intercore distance is small, as is the case for the atomistic segments. As a result, one or both cores have to rotate until the first beads leave the thin inter-core slice. Core adjustment increases the time required for cores escaping the "cages" formed by neighboring cores. In atomistic models, only the segment adjustment is necessary – the first segment can be stretched and laid down to the surface to pass through the inter-particle slice. In NOHMs grafted with long chains, reduced core volume fraction reduces the number of neighboring nanoparticle pairs, as reflected by lower $g_{cc}(r)$ peaks in the bottom panel of Fig. 4. That means that a smaller number of cores are frustrated by the caging effects and thus the acceleration caused by decreased friction dominates the dynamical behavior (see Fig. 8 bottom panel).

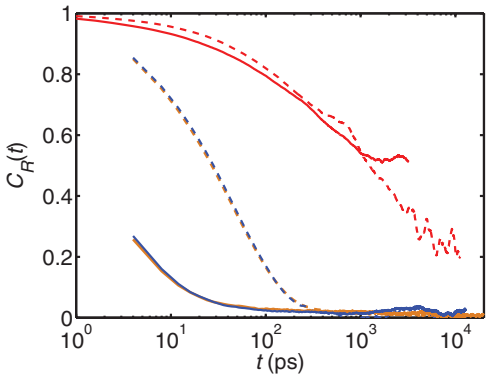

FIG. 9. Correlation functions of segment-to-segment distances for NOHMs grafted with pentamers or 3-bead chains (solid lines) and NOHMs grafted with tridecamers or 7-bead chains (dashed lines). Red lines: atomistic systems; orange lines: coarse-grained NOHMs using uncorrected inter-core potentials; blue lines: coarse-grained NOHMs using corrected inter-core potentials.

We can obtain an estimate for the contribution from the core-core potential changes to the energy boost, $\langle \Delta V_{\text{b}}\rangle$ in Eq. (1), caused by switching the atomistic description of cores to coarse-graining descriptions. $\langle \Delta V_{\text{b}}\rangle$ is the difference between coarse-grained and atomistic energy barriers one core has to overcome when transiting from one cage to another. We denote the contributions from U_{cc} to be $\langle \Delta V_{\text{b, cc}}\rangle$ and in analogy to $\langle \Delta V_{\text{b}}\rangle$ in previous work,[25,27] the component can be estimated through

$$\langle \Delta V_{\text{b, cc}}\rangle = \int_{r=0}^{\infty} U \mathrm{d}r = \int_{r=0}^{\infty} \langle N_{cc,\,CG}(r)\rangle U_{cc,\,CG}(r)\mathrm{d}r - \int_{r=0}^{\infty} \langle N_{cc,\,at}(r)\rangle U_{cc,\,at}(r)\mathrm{d}r, \tag{4}$$

where $\langle N_{cc}(r)\rangle$ is the average number density of neighbors per core and calculated through $\langle N_{cc}(r)\rangle = g_{cc}(r)N_p/V$, where V is the simulation box volume. Unlike bulk polymers, for which only the first neighbor shell dominates the changes of energy barriers after coarse-graining,[26,27] Fig. 10 shows for NOHMs the core-core potentials and the nanoparticle distributions have significant effects on $\langle \Delta V_{\text{b, cc}}\rangle$ up to

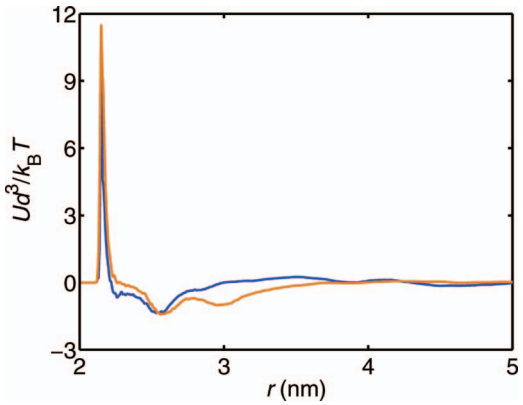

FIG. 10. Integrants of Eq. (4) for pentamer (3-bead chain) NOHMs (blue) and tridecamer (7-bead chain) NOHMs (orange).

4 nm – the second layer. Interestingly, the integration of Eq. (4) generates $\langle \Delta V_{b,cc} \rangle < 0$ for both NOHMs shown in Fig. 10, suggesting that switching particle-particle potential in atomistic NOHMs to coarse-grained core-core potential in coarse-grained models has a slow-down effect on NOHMs diffusion. Since the NOHMs do not only interact with their neighboring cores, but also with their grafted chains, the actual speed-up of NOHMs relies on the combination of the component contributions from the changes of U_{cc}, U_{cb}, and U_{bb}. The total energy boost should be $\langle \Delta V_b \rangle = \sum_{\alpha,\beta} \langle \Delta V_{b,\alpha\beta} \rangle (\alpha, \beta = c, b)$. U_{bb} has been shown to produce a positive $\langle \Delta V_b \rangle$ and accelerate bead motions in bulk polymers composed by single type of united atoms or beads.[27] It is then natural to conclude that with longer grafted chains, U_{bb} contributes more to $\langle \Delta V_b \rangle$ compared with U_{cc} and therefore coarse-grained NOHMs with longer chains diffuse faster than in atomistic models. To verify contributions from different components, a more strict estimation is needed for the differences between cage-escape energy barriers between atomistic and coarse-grained models.

IV. CONCLUSIONS

This work focused on multiscale modeling of poly(ethylene oxide) oligomers and PEO oligomer-grafted silica nanoparticles (NOHMs), with emphasis on how structure-based coarse-graining modifies the dynamics of the system. With softer interactions, the diffusion of coarse-grained PEO oligomers in melt are accelerated and the speed-ups depend on chain lengths and temperature. Around room temperature, coarse-graining shortens the "oligomer" regime; at high temperatures, the chain length dependence of diffusion coefficients of coarse-grained oligomers obeys the same scaling law as atomistic PEO chains. Similarly, the coarse-grained grafted chains of NOHMs show faster relaxation than the atomistic grafted PEO oligomers. However, the core motions are very sensitive to the coarse-grained inter-core potentials. Short-chain NOHMs have slower cores after being coarse-grained, whereas the cores of long-chain grafted nanoparticles diffuse faster similar to the effect coarse-graining has on linear chain systems. Grafting topology is one cause of the anomalous dynamic changes of NOHMs before and after coarse-graining. In addition, a simple transition-state estimation suggests not all softer potentials developed based on structure-based mapping generate speed-up effects on dynamics.

The complexity of the atomistic grafted-nanoparticle model used in this study limits the number of structural parameters and thermal conditions that can be studied in detail. To have a systematic investigation and to simplify the analysis of effects of $U_{cb,at}$ and $U_{bb,at}$ on the structure and dynamics, it would be more helpful to investigate simpler systems. For example, a simplified grafted-particle system, i.e., spherical particles and chains formed by connecting uniform atoms with only bonds and its coarse-grained model, provides a good starting point. Star polymers, where the size of the central emanating point is negligible compared to the overall molecule size, are another interesting set of structures. Direct coarse-graining unphysically increases the size and the stiffness of the center. Starting from grafted particles, whose atomistic models already have finite sizes at the central point, and extrapolating to small cores may provide an alternative to explore coarse graining of star polymers.

We have discussed in Sec. III the sensitive dependence on inter-core potentials of the structural distributions and dynamics of cores, and its negative effects on the computational efficiency of coarse-grained models. One direction for future research is to develop a predictive way to find the inter-core potentials that can generate correct structural distributions, avoiding the time-consuming iterations for core-core potential construction for each altered conditions. The sensitivity of dynamics to coarse-graining is well-established in multiscale modeling, resulting in accelerated diffusion of small molecules and linear polymers. As shown here, in grafted-topology systems there exists the possibility that softer potentials slow down the diffusion. Dynamic rescaling methods, in particular, the Mori-Zwanzig formalism, having been applied to solids,[50] linear chain liquids,[51] etc., can be used to correct the dynamics for grafted nanoparticles. By adding dissipative forces arising from eliminated internal degrees of freedoms, the method recovers the dynamics at long time when the internal motions are relaxed. The challenges lie in the determination of the friction coefficient, which is usually not transferrable to different thermodynamic conditions or different chemical environments. Lyubimov derived an analytical approach to estimate the friction coefficients for linear chains composed of only one type of coarse-grained beads.[51] With still a long way to go to approach real systems, these works point out a possible direction for solution of the issues identified in the present study.

ACKNOWLEDGMENTS

This publication is based on work supported in part by Award No. KUS-C1-018-02, made by King Abdullah University of Science and Technology (KAUST). Additional support was provided by Grant No. CBET-1033155 from the U.S. National Science Foundation (NSF).

[1] P. Agarwal and L. A. Archer, Phys. Rev. E **83**, 041402 (2011).
[2] J. Nugent, S. S. Moganty, and L. A. Archer, Adv. Mater. **22**, 3677 (2010).
[3] K.-Y. Lin and A.-H. A. Park, Environ. Sci. Technol. **45**, 6633 (2011).

[4]E. Hackett, E. Manias, and E. P. Giannelis, Chem. Mater. **12**, 2161 (2000).
[5]D. Brown, P. Mélé, S. Marceau, and N. D. Albérola, Macromolecules **36**, 1395 (2003).
[6]D. Barbier, D. Brown, A.-C. Grillet, and S. Neyertz, Macromolecules **37**, 4695 (2004).
[7]D. Brown, V. Marcadon, P. Mélé, and N. D. Albérola, Macromolecules **41**, 1499 (2008).
[8]T. V. M. Ndoro, E. Voyiatzis, A. Ghanbari, D. N. Theodorou, M. C. Böhm, and F. Müller-Plathe, Macromolecules **44**, 2316–2327 (2011).
[9]B. B. Hong and A. Z. Pianagiotopoulos, J. Phys. Chem. B **116**, 2385 (2012).
[10]L. Khounlavong, V. Pryamitsyn, and V. Ganesan, J. Chem. Phys. **133**, 144904 (2010).
[11]P. K. Depa and J. K. Maranas, J. Chem. Phys. **126**, 054903 (2007).
[12]T. B. Martin, A. Seifpour, and A. Jayaraman, Soft Matter **7**, 5952 (2011).
[13]V. Pryamtisyn, V. Ganesan, A. Z. Panagiotopoulos, H. J. Liu, and S. K. Kumar, J. Chem. Phys. **131**, 221102 (2009).
[14]Q. H. Zeng, A. B. Yu, and G. Q. Lu, Prog. Polym. Sci. **33**, 191 (2008).
[15]J. Kalb, D. Dukes, S. K. Kumar, R. S. Hoy, and G. S. Grest, Soft Matter **7**, 1418 (2011).
[16]A. Chremos and A. Z. Panagiotopoulos, Phys. Rev. Lett. **107**, 105503 (2011).
[17]A. Chremos, A. Z. Panagiotopoulos, and D. L. Koch, J. Chem. Phys. **136**, 044902 (2012).
[18]A. Chremos, A. Z. Panagiotopoulos, H.-Y. Yu, and D. L. Koch, J. Chem. Phys. **135**, 114901 (2011).
[19]S. Goyal and F. A. Escobedo, J. Chem. Phys. **135**, 184902 (2011).
[20]Y. Fujii, Z. H. Yang, A. Clough, and O. K. C. Tsui, Macromolecules **43**, 4310 (2010).
[21]S. T. Knauert, J. F. Douglas, and F. W. Starr, J. Polym. Sci., Part B: Polym. Phys. **45**, 1882 (2007).
[22]N. Lacevic, R. H. Gee, A. Saab, and R. Maxwell, J. Chem. Phys. **129**, 124903 (2008).
[23]G. D. Smith, D. Bedrov, L. Li, and O. Byutner, J. Chem. Phys. **117**, 9478 (2002).
[24]P. Carbone, H. A. K. Varzaneh, X. Y. Chen, and F. Müller-Plathe, J. Chem. Phys. **128**, 064904 (2008).
[25]D. Fritz, K. Koschke, V. A. Harmandaris, N. F. A. vander Vegt, and K. Kremer, Phys. Chem. Chem. Phys. **13**, 10412 (2011).
[26]P. Depa, C. X. Chen, and J. K. Maranas, J. Chem. Phys. **134**, 014903 (2011).
[27]P. K. Depa and J. K. Maranas, J. Chem. Phys. **123**, 094901 (2005).
[28]J. Fischer, D. Paschek, A. Geiger, and G. Sadowski, J. Phys. Chem. B **112**, 13561 (2008).
[29]H. Lee, A. H. de Vries, S.-J. Marrink, and R. W. Pastor, J. Phys. Chem. B **113**, 13186 (2009).
[30]R. M. Cordeiro, F. Zschunke, and F. Müller-Plathe, Macromolecules **143**, 1583 (2010).
[31]D. Bedrov, J. Chem. Theory Comput. **2**, 598 (2006).
[32]S. Nielsen, C. F. Lopez, G. Srinivas, and M. L. Klein, J. Phys.: Condens. Matter **16**, R481 (2004).
[33]A. F. Voter, Phys. Rev. Lett. **78**, 3908 (1997).
[34]C. F. Lopez, S. O. Nielsen, P. B. Moore, J. C. Shelley, and M. L. Klein, J. Phys.: Condens. Matter **14**, 9431 (2002).
[35]B. B. Hong, E. Fernando, and A. Z. Panagiotopoulos, J. Chem. Eng. Data **55**, 4273 (2010).
[36]A. K. Soper, Chem. Phys. **202**, 295 (1996).
[37]D. Reith, M. Pütz, and F. Müller-Plathe, J. Comput. Chem. **24**, 1624 (2003).
[38]A. P. Lyubartsev and A. Laaksonen, Phys. Rev. E **52**, 3730 (1995).
[39]T. Murtola, A. Bunker, I. Vattulainen, M. Deserno, and M. Karttunen, Phys. Chem. Chem. Phys. **11**, 1869 (2009).
[40]M. S. Shell, J. Chem. Phys. **129**, 144108 (2008).
[41]A. Chaimovich and M. S. Shell, J. Chem. Phys. **134**, 094112 (2011).
[42]F. A. Escobedo and J. J. de Pablo, J. Chem. Phys. **106**, 9858 (1997).
[43]C. X. Chen, P. Depa, V. G. Sakai, J. K. Maranas, J. W. Lynn, I. Peral, and J. R.D. Copley, J. Chem. Phys. **124**, 234901 (2006).
[44]S. J. Plimpton, J. Comp. Physiol. **117**, 1 (1995).
[45]See http://lammps.sandia.gov/ for LAMMPS users manual.
[46]S. Swier, R. Pieters, and B. van Mele, Polymer **43**, 3611 (2002).
[47]D. Brown, J. H. R. Clarke, M. Okuda, and T. A. Yamazaki, J. Chem. Phys. **100**, 1684 (1994).
[48]V. A. Harmandaris and K. Kremer, Macromolecules **42**, 791 (2009).
[49]J. T. Padding and W. J. Briels, J. Phys.: Condens. Matter **23**, 233101 (2011).
[50]X. T. Li, Int. J. Numer. Methods Eng. **83**, 986 (2010).
[51]I. Lyubimov, Phys. Rev. E **84**, 031801 (2011).